Appeared in Proc. of International Joint Conference on Neural Networks (IJCNN), (Orlando, USA), August 2007

A Texture-Based Neural Network Classifier for Biometric Identification using Ocular Surface Vasculature

Reza Derakhshani and Arun Ross

***Abstract*— In an earlier work we had explored the possibility of utilizing the vascular pattern of the sclera, episclera, and conjunctiva as a biometric indicator. These blood vessels, which can be observed on the white part of the human eye, demonstrate rich and seemingly unique details in visible light, and can be easily imaged using commercially available digital cameras. In this work we discuss a new method to represent and match the textural intricacies of this vascular structure using wavelet-derived features in conjunction with neural network classifiers. Our experimental results, based on the evidence of 50 subjects, indicate the potential of the proposed scheme to characterize the individuality of the ocular surface vascular patterns and further confirm our assertion that these patterns are indeed unique across individuals.**

I. Introduction

BIOMETRICS is the science of establishing the identity of individuals based on their unique physical or behavioral attributes [1]. Compared to traditional authentication methods such as ID cards (token-based) and passwords (knowledge-based), biometric recognition is considered to be more convenient and secure since an individual's biological signatures cannot be easily lost, forgotten or stolen. Among all biometric traits, the textural structure of the human iris has been observed to be robust and reliable [2]. However, the performance of iris recognition systems is adversely affected by the quality of the acquired images. In particular, the presentation of non-frontal iris images to the system can result in inferior biometric matching performance. This has initiated research in the development of algorithms for processing off-angle, or non-ideal, iris images. However, besides the iris, human eyes carry other specific and identifiable patterns. One such pattern arises from the layers of vasculature seen on the white part of the eyeball. Most notably, when the camera acquires a non-frontal image of the iris, vascular information of the sclera, episclera, and conjunctiva is revealed, offering a complementary source of biometric information in addition to the iris under this otherwise challenging pose. Incorporation of this modality in existing iris systems can also decrease the threat of spoof attacks as duplication of such intricate microcirculation by physical artifacts is expected to be non-trivial.

In an earlier publication, we had introduced the use of this ocular surface vasculature as a biometric and had presented some preliminary results in this regard [3]. In this work, we describe a new feature extraction and matching algorithm that treats the aforementioned vasculature as a textural entity rather than a landmark-rich structure composed of bifurcating points. The proposed feature extraction and matching scheme is evaluated on an extended dataset comprising of a larger pool of subjects, some of whom provided data over a longer period of time

II. Ocular Surface Vasculature

Using vascular patterns for personal identification has been studied in the context of fingers [4], palm [5], and retina [6]. In the case of retinal biometrics, which is closely related to the new modality discussed here, a special optical device for imaging the back of the eyeball is needed. Due to its perceived invasiveness and the required degree of subject cooperation, the use of retinal biometrics may not be acceptable to some individuals.

The conjunctiva is a thin, transparent, and moist tissue that covers the outer surface of the eye, including the white of the eye (sclera), as well as the inner lining of the eyelid. The part of the conjunctiva that covers the inner lining of the eyelids is called palpebral conjunctiva, and the part that covers the outer surface of the eye is called ocular (or the bulbar) conjunctiva, which is of our interest. The ocular conjunctiva is very thin and clear; thus the vasculature (including those of the episclera and sclera) is easily visible through it. The layers of visible surface microcirculation yield a rich and complex network of fine veins (Fig. 1). From this point on, we will simply refer to all the visible vascular structures on the white of the eye as conjunctival vasculature. The apparent complexity and specificity of these vascular patterns motivated us to study their potential as personal identifiers [7]. It is interesting to note that humans are the only mammals with extensive exposed sclera, which is amenable to imaging of the encompassing conjunctival vasculature [8].

Manuscript received February 12, 2007. This work was supported in part by a grant from the Center for Identification Technology Research (CITeR), an NSF IUCRC center at West Virginia University, Morgantown, WV.

Reza Derakhshani is with the Department of Computer Science and Electrical Engineering, University of Missouri-Kansas City, Kansas City, MO 64110 USA (phone: 816-235-5338; fax: 816-235-5159; e-mail: reza@umkc.edu).

Arun Ross is with the Lane Department of Computer Science and Electrical Engineering, West Virginia University, Morgantown, WV 26506 USA (Arun.Ross@mail.wvu.edu).

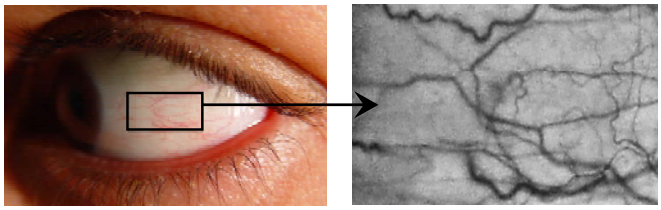

Fig. 1. Enhanced close up of ocular surface vasculature.

Based on our pilot study on 50 volunteers, and related discussions in the literature, we have found conjunctival vasculature to be a suitable candidate for biometric identification as it conforms to the following criteria [9]:

(a) As living tissue, the white part of the eye along with its transparent skin has conjunctival vasculature (*universality criterion*).

(b) Vasculature is created during embryonic vasculogenesis. Its detailed final structure is mostly stochastic and thus its uniqueness stands to reason. Even though no exhaustive uniqueness study of vascular structures has been conducted, studies on specific surfaces such as the eye fundus have confirmed the uniqueness of their vascular patterns, even between identical twins [10], [11] (*uniqueness criterion*).

(c) Other than cases of significant trauma, pathology, or biochemical interference, spontaneous adult ocular vasculogenesis and angiogenesis usually do not occur. Hence, we expect the conjunctival vascular structure to have reasonable stability [12] (*permanence criterion*).

(d) Conjunctival vasculature can be captured with commercial off the shelf digital cameras, making this modality highly practical (*practicality criterion*).

(e) Since the subjects are not required to stare directly into the camera lens for conjunctival captures, and given the possibility of photographing conjunctival vasculature from several feet away, our suggested modality is non-intrusive and more convenient for the user (*acceptability criterion*).

(f) The fine, multi-surface structure of the ocular veins makes them hard to reproduce as a physical artifact (*non-circumventability criterion*).

Besides its demonstrated capabilities as a stand-alone biometric modality, we anticipate that the addition of conjunctival biometrics will increase the utility and precision of the current iris-based systems as well, especially under the following circumstances: (i) the subject is not cooperative (e.g. subject will not hold steady for iris registration, or he/she is looking away from the camera); (ii) subject's iris cannot be successfully enrolled as a result of trauma, surgical alteration, or other pathological disfigurations; and (iii) the capture is long-range or otherwise non-ideal, where the iris images provide less information and need to be augmented with other identifiable features.

III. Processing Methods

A. Image Capture

The conjunctival vasculature can be imaged when an individual is "looking straight into the camera", "looking to the left", "looking to the right", or "looking up". Such captures are not amenable to the "looking-down" pose due to the resulting natural drop of the upper eyelid. These poses, individually or collectively, can be used for conjunctival biometric authentification.

For this study, we obtained regular digital eye images of 50 volunteers (institutional review board protocol UMKC AHS IRB 06-22e), using a Cannon® 20D digital SLR camera with EFS 60mm f/2.8 Macro and EF 70-200 mm f/4L USM telephoto lenses. We captured digital images of the volunteer eyes under the aforementioned gaze directions and from three distances: 30 cm (or 1 ft, with macro lens) and 152 and 274 cm (or 5 and 9 ft, with telephoto lens). This procedure was repeated twice for each volunteer, with an approximate 20 minute lapse in between, resulting in 2 sets of images. The "looking to the left" and "looking to the right" poses of the first set of images were used for registering the individuals' conjunctival vasculature biometrics (and later used for classifier training). A similar second series of shots were used to produce the corresponding biometric authentication results (i.e. for classifier testing). The eye captures were segmented manually from the face images. However, we used a simple intensity-based routine to further segment the image into scleral regions of interest, which were the rectangular areas of the white of the eye and to the left and right of the iris. . We used the MATLAB®7 software running on x86-based desktop computers for all the computations.

B. Image Preprocessing

After the extraction of target conjunctival areas, a gray-level image was produced by separating the green layer of the original RGB captures, which has been known to yield the best "red-free" vascular image [13],[14]. Next, we performed a contrast-limited adaptive histogram equalization to further accentuate segmented images of the conjunctival vasculature (Fig. 2). Here, we divided target segments of conjunctival images, on the left and right of the iris, into 8×8 tiles each for better localized enhancement. We chose 256-bin histograms for limited contrast enhancement on each tile (uniform intensity distribution adjustment).

C. Feature Extraction

Image compression techniques such as Discrete Cosine Transform (DCT) and Wavelet-based methods have been successfully used as feature extractors for neural network-based image classifiers in other contexts [15],[16]. For this application, and based on our experiments with our current dataset in terms of different DCT and Wavelet-based features, we found certain types of Wavelet-based features to perform slightly better with a feed-forward neural

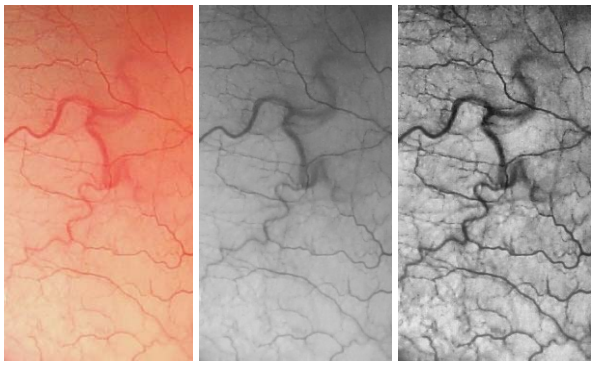

Fig. 2. Image preprocessing. Left: segmented conjunctival area (RGB image under normal indoor lighting); middle: the gray scale image obtained from the green layer; right: the green layer image after adaptive histogram equalization.

network classifier. Note that for data-driven nonlinear classifiers such as neural networks, it might be better to co-design the feature extractor with the classifier to better accommodate nonlinearly separable disjoint classes in the feature space.

Based on experiments with our classifier and data, we utilized Discrete Cohen-Daubechies-Feauveau 9/7 Wavelet transform, CDF 9/7, which is an effective biorthogonal Wavelet used in JPEG2000 and FBI fingerprint compressions [17]. Using the conjunctival segments present to the left and right of the iris, and after the earlier-mentioned preprocessing, we concatenated and down-sampled the mosaicked image to 100×200 pixels, and then performed a two dimensional CDF 9/7 transforms on the result. We used the transform with 8 levels and retained the first 512 components of the results (from the first 16×32 block) as the feature vector for each eye capture (subject's biometric template). This is essentially an efficient lossy compression of the target vascular segments and thus retains most of the textural information of the conjunctival patterns in a relatively small feature vector (see Fig. 3).

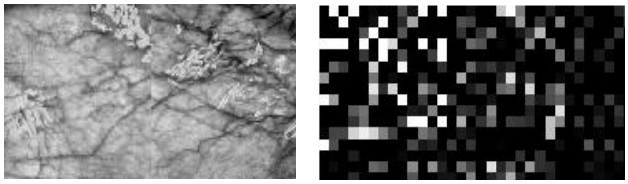

Fig. 3. Left: an input image obtained by mosaicking the scleral regions to the left and right of the iris. Right: the resulting CDF 9/7 wavelet feature matrix (16×32=512 features).

D. Classification

For testing, the claimant's template needs to be matched against his or her stored template for verification (one-to-one matching), or against the whole database of templates for identification (one-to-many matching). Based on their nonparametric, data-driven discrimination capabilities on datasets with unknown distributions [18], and their reported successful applications in biometric identification (e.g. see [19]), we used a single hidden layer feed forward neural network as our classifier. Based on our 512 feature, 50 user database, we chose a network with 512 input nodes, 300 hidden nodes, and 50 output nodes with bi-valued targets and hyperbolic tangent nonlinearities. We trained our network using enrollment data (first capture series) from all the three distances and with scaled conjugate gradient algorithm [20], which provides a good balance between performance, speed, and memory requirements. We tested the performance of the trained neural network classifier against the unseen second series of captures. Given the scarsity of training data in many biometric applications, we chose a regularized error function given in (1) to penalize extraneous weights and, thus, avoid over-parameterization in absence of robust validation-based early stopping:

$$SSE_{\text{Regularized}} = \frac{1}{2}\sum_{i=1}^{N} e_i^{\,2} + \frac{\lambda}{2}\sum_{k=1}^{P} w_k^{\,2} \quad (1)$$

Here N is the total number of training samples, e_i is the classification error for i^{th} capture, P is the total number of free parameters (i.e. network weights w_k), and λ is the regularization constant which was set to 0.2 in our experiments. This parameter dictates the weight decay pressure, which is the result of weight-shrinking gradient of the second term in (1). Under gradient descent learning, lowering the above sum of squared errors (SSE) will yield sparse and thus low variance models on limited training datasets with good generalization capabilities. Another justification of the above augmented error criterion comes from derivation of (1) via a Bayesian framework and assuming Gaussian distribution for both the neural network weights and target data noise [21]. Either way, our post-training inspection of Hinton maps showed the utility of the above regularization scheme in reducing the effective number of network weights (Fig. 4).

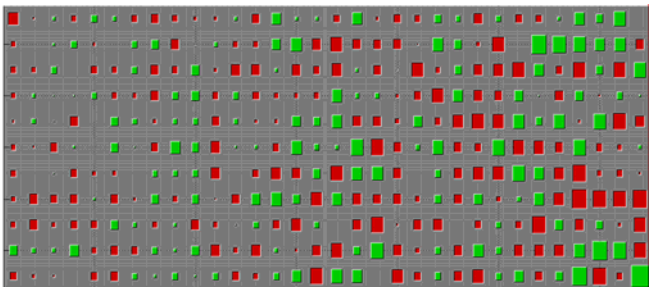

Fig. 4. A sample Hinton map showing the input receptive field of a neuron (from 16×32 Wavelet features) in the trained classifier. The area of each square is proportional to the connection weight it represents, and the color denotes the corresponding sign (red/dark denotes negative, and green/light denotes positive).

IV. Results and Discussions

We evaluated the trained neural network using the unseen test images (i.e. the second series of captures). The results

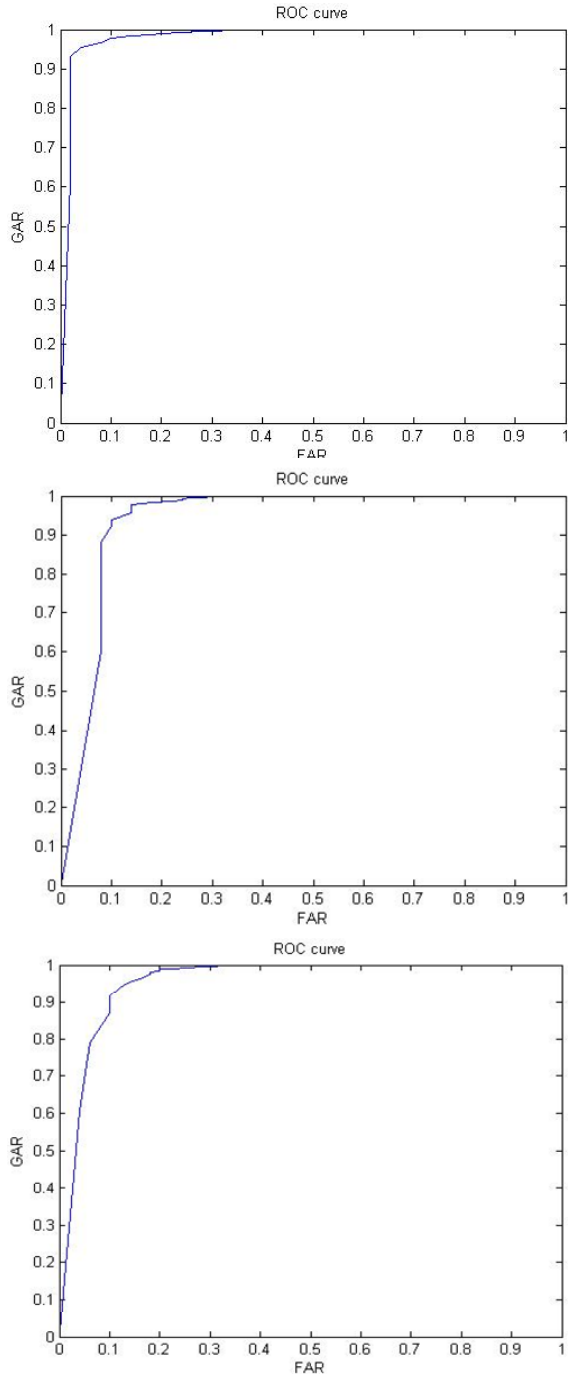

Fig 5. ROC curves of test data and for multi-distance conjunctival vasculature matching, using both eyes. Top: 1 ft distance, 4.3% EER; middle: 5 ft distance, 8.8% EER; and bottom: 9 ft distance 9.2% EER.

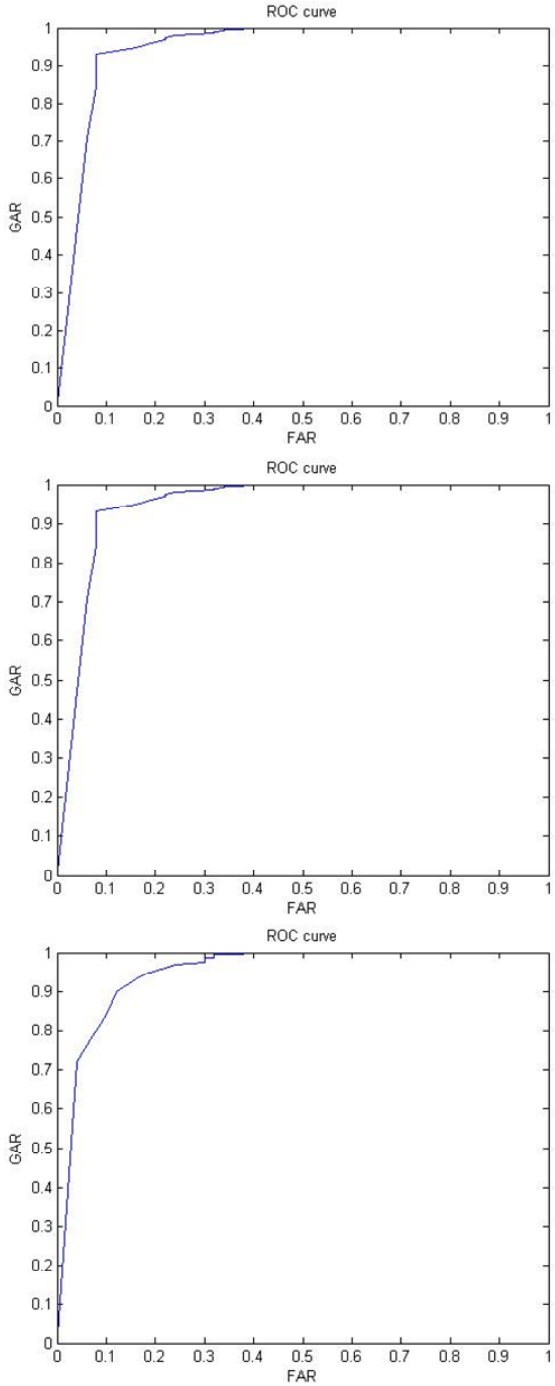

Fig 6. ROC curves of test data and for multi-distance conjunctival vasculature matching, using one eye. Top: 1 ft distance, 6.5% EER; middle: 5 ft distance, 7.4% EER; and bottom: 9 ft distance 11% EER.

are depicted here using Receiver Operating Characteristics (ROC) curves for 50 subjects, which are obtained by plotting the Genuine Accept Rate (GAR) against the False Accept Rate (FAR) and by changing the decision threshold applied to the neural network's continuous outputs. Fig. 5 shows test ROC curves using conjunctival vasculature data from both eyes and for our 50-subject unseen test data. For ease of comparison, we are also reporting the Equal Error Rate (EER) of these curves. EER is simply the error rate when GAR=FAR. As can be seen from Fig. 5, when using conjunctival images from both eyes, the EERs are 4.3% for near distance images (1 ft), 8.8% for medium distance images (5 ft), and 9.2% for long distance images (9 ft). The performance degraded slightly when we trained and tested our neural network using conjunctival vasculature images of only one eye per subject, yielding 6.5%, 7.4%, and 11%

EERs, respectively, for 1, 5, and 9 ft test data (Fig. 6).

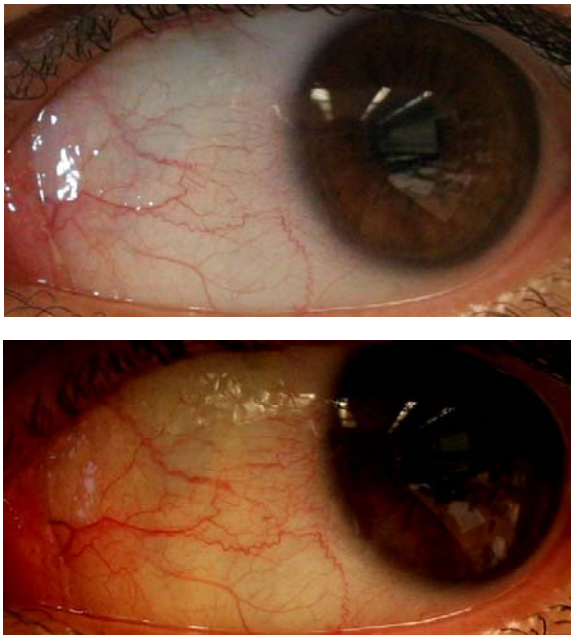

Fig 7. An example of conjunctival vasculature's temporal invariance. Top: initial enrollment image; bottom: the same eye after 17 weeks. Note the varying glare due to unrestricted, regular indoor lighting.

After 4 months from the first data collection, 17 of the 50 volunteers came back for a long term study of their conjunctival vasculature patterns. A close visual inspection of time-lapsed images revealed no significant change in the conjunctival vasculature patterns, indicating temporal pattern invariance to the extent that the limits of this initial study allow (Fig. 7).

We also tried to inspect another potential caveat regarding our new biometric modality. From the list of most probable adverse chemical agents to this measure, we chose to study the effects of over the counter Tetrahydrozoline HCL-based redness relievers such as Visine®, Eye-Lite®, and Readycor® with blanching effects on the conjunctival vasculature of interest. Based on the conjunctival images of three volunteers that used regular Visine®, we found no significant change in the conjunctival vascular patterns, especially after our enhancement routine (Fig. 8).

One can categorize the sources of observed error in this study as those induced by adverse lighting (glare), photography (equipment and human operator error), and image segmentation. A closer look at our current dataset reveals significant amount of variable glare, which was the result of an original stipulation not to use any special lighting arrangements. Thus, we conjecture that our primary source of error is adverse lighting that impacts the subsequent segmentation and feature extraction routines.

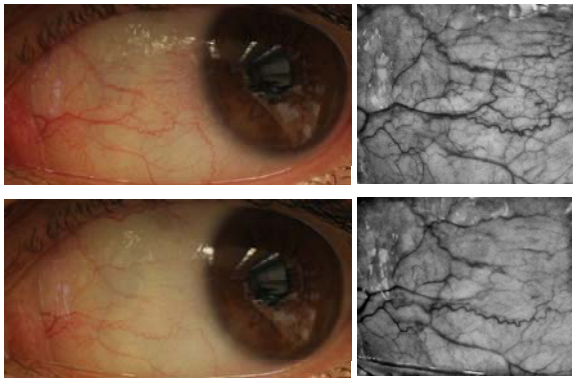

Fig 8. An example of conjunctival vasculature's resilience to redness-reliever eye drops. Top-left: before the application of Visine®; bottom-left: after the application of the mentioned eye drop. The right column shows corresponding preprocessed, enlarged areas for comparison. Note how most of the vascular structures are still visible despite the blanching effect of the eye drops.

V. Conclusions and Future Work

We have introduced a texture-based classification scheme for our novel conjunctival vasculature biometrics. Using the established Wavelet-derived features and neural network classifiers for a new application domain, we have shown the potential of conjunctival biometrics as a standalone authentification system using ordinary photographic setup. This new biometric modality also has the potential of adding precision and security to existing iris biometric systems. The corresponding research on the fusion of iris and conjunctival scans is on our future agenda. We also wish to incorporate alternate and complementary techniques of conjunctival feature extraction and matching, including the fusion of our previous minutiae-based approach [3] with the current texture-based system for a robust, multi-algorithmic approach. We hypothesize the different nature of these methods should produce part-uncorrelated identification score errors and thus a committee of the aforementioned classifiers might yield lower error rates.

Our research also shows potential for long range ocular biometrics with our current results indicating the possibility of conjunctival identification from up to 3 meters away. The performance of our system on longer distances is the subject of future research.

We have observed minimal visible conjunctival vasculature variance over a course of 4 months, but we wish to extend our invariance study over longer periods of time for further insight into possible template aging. We also wish to study larger groups of subjects and under different circumstances, including possible pathologies such as conjunctivitis (pink eye) and spoofing scenarios.

ACKNOWLEDGMENT

The authors wish to thank Dr. Rohit Krishna (UMKC Medical School) for his invaluable suggestions and contributions. We are also grateful for the assistance of Ashish Anand (graduate research assistant, CSEE, UMKC) for acquiring and processing the study images. The CDF 9/7 Wavelet MATLAB® code was developed and made available by Pascal Getreuer [22].

REFERENCES

[1] A. K. Jain, R. Bolle, and S. Pankanti (Eds), *BIOMETRICS: Personal Identification in Networked Society*, Kluwer Academic Publishers, 1999.

[2] J. G. Daugman, , "High confidence visual recognition of persons by a test of statistical independence," IEEE Transactions on Pattern Analysis and Machine Intelligence, vol. 15, no. 11, pp. 1148–1160, 1993.

[3] R. Derakhshani, A. Ross, and S. Crihalmeanu, "A new biometric modality based on conjunctival vasculature", Proceedings of ANNIE, St. Louis, MO, November 2006.

[4] N. Miura, A. Nagasaka, and T. Miyatake, "Feature extraction of finger vein patterns based on iterative line tracking and its application to personal identification," Systems and Computers in Japan, vol. 35, pp. 61–71, 2004.

[5] C. L. Lin, and K. C. Fan, "Biometric verification using Thermal images of palm-dorsa vein patterns," IEEE Transactions on Circuits and Systems for Video Technology, vol. 14, pp. 199–213, 2004.

[6] R. Hill, "Retina Identification," Chapter 4 in A., Jain, Bolle, and S., Pankanti, *BIOMETRICS: Personal Identification in Networked Society,*" 2nd Printing, Kluwer Academic Publishers, 1999.

[7] R. Derakhshani, and A. Ross, "Conjunctival scans for personal identification", provisional patent filed May 2005, File No. 05UMK074, full disclosure filed in May 2006 (pending).

[8] H. Kobayashi and S. Kohshima, "Unique morphology of the human eye," Nature, Vol. 387, No. 6635, pp. 767-768, 1997.

[9] A. K. Jain, A. Ross, and S. Prabhakar, " An introduction to biometric recognition", IEEE Transactions on Circuits and Systems for Video Technology, Special Issue on Image and Video-Based Biometrics, vol. 14, No. 1, pp. 4-20, 2004.

[10] C. Simon, and I. Goldstein, "A new scientific method of identification," New York State Journal of Medicine, vol. 35, No. 18, pp. 901-906, 1935.

[11] P. Tower, "The fundus Oculi in monozygotic twins: Report of six pairs of identical twins," Archives of Ophthalmology, vol. 54, pp. 225-239, 1955.

[12] A. M. Joussen, "Vascular plasticity - the role of the angiopoietins in modulating ocular angiogenesis," Graefe's Archive for Clinical and Experimental Ophthalmology, vol. 239, Issue 12, pp. 972 - 975, 2001.

[13] Rohit Krishna M.D., personal communications, University of Missouri-Kansas City, 2005.

[14] C.G. Owen, T. J. Ellis, A.R. Rudnicka, and E.G. Woodward "Optimal green (red-free) digital imaging of conjunctival vasculature." Ophthalmic Physiol Opt. 22(3):234-43, 2002.

[15] Z. Pan, A. Rust, and H. Bolouri, "Image redundancy reduction for neural network classification using discrete cosine transforms," in Proceedings of the International Joint Conference on Neural Networks, vol. 3, Como, Italy, pp. 149-154, 2000.

[16] T. Randen and J.H. Husoy, "Filtering for texture classification: a comparative study," Pattern Analysis and Machine Intelligence, IEEE Transactions on , vol.21, no.4pp.291-310, Apr 1999.

[17] Dong Wei; Jun Tian; Wells, R.O., Jr.; Burrus, C.S., "A new class of biorthogonal wavelet systems for image transform coding," Image Processing, IEEE Transactions on , vol.7, no.7pp.1000-1013, Jul 1998

[18] S. Haykin, Neural Networks: A Comprehensive Foundation. Prentice Hall, 1994.

[19] L. C. Jain et al (Eds): Intelligent Biometric Techniques in Fingerprint and Face Recognition. CRC Press International, 1999.

[20] M. F. Møller: A Scaled Conjugate Gradient Algorithm for Fast Supervised Learning. Aarhus University Publishing, Denmark, 1990.

[21] C. M. Bishop: Pattern Recognition and Machine Learning. Springer, 2006.

[22] MATLAB® online community at http://www.mathworks.com/matlabcentral/fileexchange/loadFile.do?objectId=6449